

Graph Edits for Counterfactual Explanations: A comparative study

Angeliki Dimitriou^{[0009-0001-5817-3794]*}, Nikolaos Chaidos^{[0009-0006-0347-2785]*}, Maria Lympertaiou^[0000-0001-9442-4186], and Giorgos Stamou^[0000-0003-1210-9874]

National Technical University of Athens `gstam@cs.ntua.gr`
`{nchaidos,angelikidim,marialymp}@ails.ece.ntua.gr`
 * These authors contributed equally

Abstract. Counterfactuals have been established as a popular explainability technique which leverages a set of minimal edits to alter the prediction of a classifier. When considering conceptual counterfactuals on images, the edits requested should correspond to salient concepts present in the input data. At the same time, conceptual distances are defined by knowledge graphs, ensuring the optimality of conceptual edits. In this work, we extend previous endeavors on *graph edits as counterfactual explanations* by conducting a comparative study which encompasses both supervised and unsupervised Graph Neural Network (GNN) approaches. To this end, we pose the following significant research question: should we represent input data as graphs, which is the optimal GNN approach in terms of performance and time efficiency to generate minimal and meaningful counterfactual explanations for black-box image classifiers?

Keywords: Counterfactual Explanations · Black-box Explanations · Scene Graphs · Graph Neural Networks · Graph Autoencoders.

1 Introduction

In the era of large and complex neural models, ensuring trust between them and humans becomes a critical issue. Explainability literature suggests a variety of methods to probe neural models behaviors, either requiring access to their inner workings [11,31] or not [6,7,10]. There is also ample discussion regarding the nature of the features involved in a human-understandable explanation; for example, low-level features e.g. pixel-related characteristics (brightness, contrast) may be unable to provide a meaningful explanation to the end user, despite being informative for a neural model [29]. This observation is applicable in the counterfactual explanation scenario, suggesting that semantics are fundamentally essential to meaningful counterfactual explanations [4,23]. In the meanwhile, both high-level semantics as well as low-level features can be expressed in the same mathematical format (e.g. numerical vectors), allowing the transition to semantically rich explanation systems [6]. In the interest of explaining visual classification systems, and with respect to recent related work [2,6,7,10,11,31], we base our current study on *conceptual counterfactual explanations*.

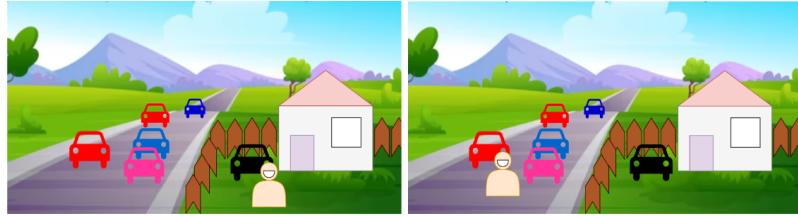


Fig. 1: Left - person in front of parked car (safe). Right - person in front of moving cars on the highway (unsafe). The relationship between the person, the car and the highway is critical for the transition to the counterfactual class.

With regard to the model accessibility an explainability system can have, most related counterfactual explanation methods belong to the white-box category [2,11,31], offering insights tailored to the model under investigation. However, in the emergence of powerful, yet proprietary models, such as ChatGPT [25] and GPT-4 [26] which are currently accessible only through APIs, black-box explanations resurface as more viable and universal solutions, able to approach a model by scrutinizing their outputs. Under these constraints, we stay within the *black-box* setting of conceptual counterfactuals [6,7,10].

We also acknowledge the importance of intra-concept roles, as associations between the same concepts via roles may result in different interpretations of situations (Figure 1). Thus, we advocate image representation via scene graphs. To this end, we extend the framework of [7] to accommodate a larger spectrum of Graph Machine Learning algorithms to serve conceptual counterfactual explanations on scene images. We retain the brute-force calculation of Graph Edit Distance (GED)[30] as the ground truth counterfactual measure, under which the closest scene graph in terms of GED belonging to a different class is considered as the “gold” counterfactual graph. In order to overcome the computational complexity of GED calculation, we employ Graph Machine Learning algorithms, such as Graph Kernels, Graph Autoencoders (GAEs) and supervised Graph Neural Networks (GNNs), which are lightweight and significantly faster than the NP-hard deterministic GED calculation [35], even when optimizations are employed [14]. Graph edits serving as counterfactual explanations are instructed via concept distances in existing hierarchies, in our case being WordNet [22]. Merits of such explanations include but are not limited to actionability, a crucial quality of counterfactuals in several domains [21]. The outline of our approach is presented in Figure 2. Overall, we explore the capabilities of Graph Machine Learning algorithms, contributing to the following:

- We prove quantitatively and qualitatively that both unsupervised (GAEs) and supervised (GNNs) methods can provide meaningful and accurate conceptual counterfactuals, viewing models under explanation as black-boxes.
- We demonstrate the trade-offs between unsupervised vs supervised approaches towards counterfactual explanations, and provide insights on the advantages of each method.

2 Related work

Counterfactual Explanations have been established as an effective explanation method [33] should certain requirements, such as actionability and feasibility be met [28]. These principles are transferred in the field of counterfactual visual explanations, which aim to explain the behaviors of image classifiers. Most of these approaches leverage pixel-level edits, denoting regions that should be minimally changed [11,13,31] and often proceed to actually generate the targeted region by employing generative models [3,5,8,36].

Since semantics are inherently tied to human-interpretable counterfactuals [4], a diverging line of work suggests moving towards conceptual rather than pixel-level counterfactuals. The notion of explainable concepts was presented in [2], where fault-lines are utilized to drive concept edits. [1] produce conceptual counterfactuals to meaningfully explain model misclassifications. However, these approaches require some degree of access to the internals of the classifier. Minimal concept edits in a black-box fashion were proposed in [10], paving the way for knowledge-based model-agnostic visual counterfactuals. Some limitations were resolved in subsequent works, suggesting an indirect [6] or direct [7] incorporation of roles into concepts, while underlining the importance of correctly selecting data and representations to obtain proper explanations. The same idea is modified to explain hallucinations of image generation models rather than classifiers [20], highlighting the significance of universal black-box explainers.

3 Method

The focus of our current study centers on determining the minimal semantic alteration necessary for an image i to transition from being classified as A to B. Each image i in our dataset I is represented by a scene graph G_i , encapsulating semantic information, therefore forming an explanation dataset $\{i, G_i\}$, as previously outlined in [10]. Utilizing a reference image i_r and candidate scene graphs G_{i_c} , the GED is computed using an optimization approach to identify the most efficient path for semantic transformation between G_{i_r} and G_{i_c} , guided by predefined graph edit operations (Replacement, Deletion, Insertion). Semantic distances, drawn from the well-crafted WordNet [22] hierarchy, guide the choice of edits, ensuring meaningful transitions while penalizing irrelevant replacements. To accelerate GED calculations, we employ optimization techniques similar to [7], utilizing the Volgenant-Jonker (VJ) algorithm [14]. Finally, to obtain the counterfactual candidate $G_{i_{cc}}$ of the original scene graph G_{i_r} , we repeat the optimized GED calculation for each candidate G_{i_c} , where $c \in C = I \setminus \{i_r\}$, ensuring that the selected closest $G_{i_{cc}}$ belongs to class $B \neq A$, while G_{i_r} belongs to class A, formulated as:

$$i_{cc} = \arg \min_{i_c \in C} (GED(G_{i_r}, G_{i_c})), \quad G_{i_r} \in A, G_{i_c} \in B \neq A \quad (1)$$

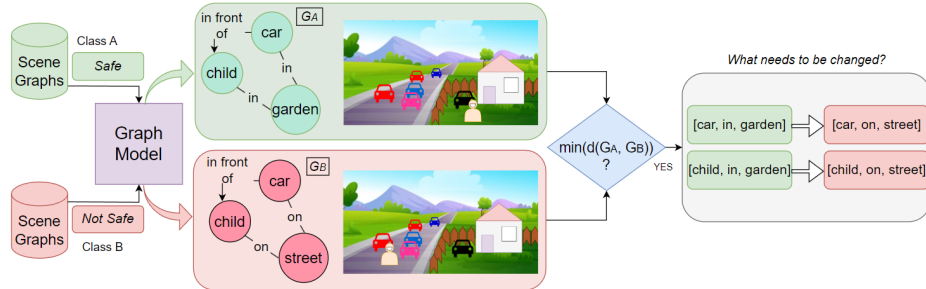


Fig. 2: Outline of our evaluation framework: Given scene graphs of classes $A \neq B$, a graph model embeds them in a low-dimensional space, allowing the retrieval of the closest graphs G_A, G_B from which we extract counterfactual edits.

3.1 The importance of Graph Machine Learning

Considering a dataset with N graphs, calculating the counterfactual $G_{i_{cc}}$ for every G_{i_r} requires $O(N^2)$ GED operations, resulting in a prohibitive calculation time, despite using optimizations. In order to accelerate this process, we leverage Graph Machine Learning algorithms to circumvent the exhaustive calculation of N^2 GEDs, accepting an unavoidable performance sacrifice.

Graph Kernels is our first step towards testing graph matching [17]. Kernels in Machine Learning are responsible for mapping the given data in high-dimensional spaces, revealing complex patterns that cannot be observed in the original dimensionality of the input data, therefore allowing the application of linear algorithms to solve non-linear problems. Graph kernels quantify the degree of similarity between subgraphs in polynomial time by employing kernel functions, thus contributing to the overall structural similarity between two given graphs. In our experiments, we will compare different graph kernel approaches.

Graph Neural Networks (GNNs) in the supervised setting comprise architectures such as Graph Convolution Network (GCN) [15], Graph Attention Network (GAT) [32], and Graph Isomorphism Network (GIN) [34]. They are incorporated in a Siamese Network to learn similarity on input instances [19], demonstrating state-of-the-art results even when trained on a smaller subset of N^2/j labeled graph pairs (N is the number of graphs in the complete dataset, j a positive integer). During training, these GNN variants learn the relationships between counterfactual graph pairs utilizing ground truth samples calculated from Eq. 1. Embedding representations on new graphs are extracted using the trained GNNs, translating graph similarity cues to distances in the embedding space, therefore allowing retrieval of counterfactual graphs $G_{i_{cc}}$ for each G_{i_r} .

Graph Autoencoders (GAEs) [16] arise as faster and more versatile solutions by eliminating the need for labeled samples, even though their metric performance often ranks lower than GNNs. GAEs implement an encoder-decoder structure, with the encoder being tasked to produce embedding representations; these representations are useful for retrieval tasks, since similarity in the embedding space corresponds to actual graph similarity. Thus, the need of GED

calculations within the training process is completely avoided, dropping the computational complexity to $O(N)$ in comparison to the $O(N^2)$ operations required in the supervised case (N is the number of graphs). The encoder and decoder modules are constructed using any of the aforementioned GNN variants (same GNN modules for the encoder and the decoder when applicable).

In all cases, we retain the NP-hard GED scores for ground truth comparison to evaluate the performance of different models on the ground-truth rank.

4 Experiments

In this experimental section, we aim to provide a thorough comparison between different kernel/GAE/GNN architectures as components of the counterfactual retrieval process. We examine them both in terms of their adherence to ground truth rankings, as well as their ability to provide minimal edits regarding both quantity and cost. Throughout this analysis, we inherently contrast supervised and unsupervised GNNs, weighing the trade-offs between employing more efficient versus accurate models and quantifying the resultant incurred damages.

4.1 Experimental setup

Data In all our experiments, we select Visual Genome (VG) [18] as the experimental dataset, due to its abundance in real-life scenes accompanied by manually annotated scene graphs. In addition, VG offers an effortless connection with WordNet, as synset annotations of objects and roles are also provided by annotators. Since graph edges are important in our analysis, we regard two density-based dataset splits for training [7]: the first one, called VG-DENSE, includes graphs with many interconnections and fewer isolated nodes. The second one called VG-RANDOM does not impose any restrictions on scene graph density. Both splits contain $N=500$ graphs. As VG does not contain ground truth scene labels we assign them using a pre-trained PLACES-365 classifier [37].

Graph Models In our study, we employ various graph kernels [24] including Shortest Path (SP), Weisfeiler-Lehman (WL), Neighborhood Hash (NH), Random Walk (RW), and Graphlet Sampling (GS), implemented using the GraKeL library. For supervised Graph Neural Network (GNN) models, we utilize single-layer siamese GCN, GAT, and GIN as described in [7], trained over 50 epochs with a batch size of 32 and Adam optimizer. Regarding Graph Autoencoders (GAEs), we implement vanilla GAE, Variational GAE (VGAE) [16], and Adversarially Regularized Variational Graph Autoencoder (ARVGA) [27], alongside a variation of Graph Feature Autoencoder (GFA) [12]. GAE and VGAE are both based on the generic auto-encoder structure, but differ in terms of loss function. ARVGA employs basic concepts from Generative Adversarial Networks to further boost the regularization of the latent embeddings produced by VGAE. Finally, GFA utilizes the Feature Decoder (whose goal is to predict the feature matrix X), alongside the original VGAE Inner-Product Decoder (whose goal is

Table 1: Counterfactual retrieval results with Supervised and Unsupervised GNN architectures. Underlined cells indicate best results per graph model (kernel, supervised, unsupervised). **Bold** denotes best results overall per dataset split.

Model	NDCG (binary)			Precision (P) (binary)			Precision (P)		
	@4	@2	@1	@4	@2	@1	@4	@2	@1
VG-DENSE									
WL kernel	0.287	0.198	0.138	0.186	0.128	0.076	0.164	0.125	0.076
SP kernel	<u>0.334</u>	<u>0.251</u>	<u>0.194</u>	<u>0.232</u>	<u>0.174</u>	<u>0.122</u>	0.154	<u>0.145</u>	<u>0.122</u>
RW kernel	0.0	0.0	0.0	0.0	0.0	0.0	0.001	0.0	0.0
NH kernel	0.282	0.192	0.131	0.124	0.086	0.05	0.088	0.073	0.05
GS kernel	0.259	0.166	0.103	0.018	0.008	0.008	0.022	0.007	0.008
Superv. GAT	0.342	0.26	0.204	0.422	0.288	0.164	0.312	0.25	0.164
Superv. GIN	0.339	0.256	0.2	0.344	0.242	0.158	0.252	0.192	0.158
Superv. GCN	0.407	0.333	0.283	0.492	0.37	0.248	0.358	0.292	0.248
GAE GAT	0.281	0.191	0.13	0.108	0.078	0.048	0.075	0.075	0.048
GAE GIN	0.281	0.191	0.13	0.132	0.098	0.052	0.082	0.078	0.052
GAE GCN	0.287	0.197	0.137	0.102	0.078	0.052	0.071	0.06	0.052
VGAE GAT	0.298	0.21	0.15	0.196	0.138	0.082	0.139	0.12	0.082
VGAE GIN	0.304	0.216	0.157	0.202	0.146	0.09	0.141	0.119	0.09
VGAE GCN	0.287	0.198	0.137	0.174	0.118	0.066	0.122	0.101	0.066
GFA GAT	0.302	0.214	0.155	0.182	0.14	0.086	0.122	0.109	0.086
GFA GIN	0.309	0.223	0.164	0.21	0.148	0.096	0.14	0.122	0.096
GFA GCN	0.163	0.165	0.158	<u>0.289</u>	<u>0.2</u>	<u>0.139</u>	0.12	0.104	0.068
ARVGA GAT	0.3	0.213	0.153	0.188	0.14	0.084	0.132	0.114	0.084
ARVGA GIN	<u>0.317</u>	<u>0.232</u>	<u>0.174</u>	0.218	0.164	0.106	0.135	<u>0.124</u>	<u>0.106</u>
ARVGA GCN	0.295	0.207	0.146	0.184	0.138	0.076	0.122	0.106	0.076
VG-RANDOM									
WL kernel	0.306	0.219	0.16	0.166	0.124	0.096	0.13	0.108	0.096
SP kernel	0.292	0.204	0.144	0.11	0.09	0.064	0.079	0.068	0.064
RW kernel	0.0	0.0	0.0	0.0	0.0	0.0	0.007	0.0	0.0
NH kernel	0.303	0.216	0.157	<u>0.168</u>	0.116	0.092	0.135	<u>0.116</u>	0.092
GS kernel	0.0	0.0	0.0	0.002	0.0	0.0	0.05	0.0	0.0
Superv. GAT	0.35	0.268	0.213	0.382	0.294	0.176	0.294	0.245	0.176
Superv. GIN	0.327	0.243	0.186	0.308	0.228	0.144	0.245	0.205	0.144
Superv. GCN	0.369	0.29	0.236	0.424	0.3	0.2	0.295	0.246	0.2
GAE GAT	0.294	0.205	0.146	0.132	0.104	0.07	0.092	0.085	0.07
GAE GIN	0.297	0.209	0.15	0.114	0.096	0.07	0.08	0.076	0.07
GAE GCN	0.291	0.203	0.143	0.114	0.1	0.066	0.079	0.078	0.066
VGAE GAT	0.305	0.218	0.159	0.16	0.122	0.09	0.103	0.1	0.09
VGAE GIN	0.304	0.217	0.158	0.152	0.118	0.088	0.11	0.101	0.088
VGAE GCN	0.303	0.216	0.157	<u>0.156</u>	0.122	0.088	0.101	0.089	0.088
GFA GAT	0.292	0.203	0.143	0.142	0.108	0.076	0.107	0.094	0.076
GFA GIN	0.298	0.211	0.151	0.142	0.11	0.082	0.11	0.093	0.082
GFA GCN	0.297	0.209	0.149	0.14	0.112	0.082	0.106	0.095	0.082
ARVGA GAT	0.305	0.218	0.159	<u>0.156</u>	<u>0.13</u>	0.092	0.111	<u>0.103</u>	0.092
ARVGA GIN	0.298	0.21	0.15	0.152	0.118	0.084	<u>0.116</u>	0.099	0.084
ARVGA GCN	<u>0.306</u>	<u>0.22</u>	<u>0.161</u>	0.154	<u>0.13</u>	<u>0.094</u>	0.113	0.097	<u>0.094</u>

Table 2: Average Number of node, edge and total edits, as well as Average Top-1 GED for counterfactual instances retrieved for VG-DENSE and VG-RANDOM.

Model	VG-DENSE				VG-RANDOM			
	Node ↓	Edge ↓	Total ↓	GED ↓	Node ↓	Edge ↓	Total ↓	GED ↓
WL kernel	5.24	11.668	16.908	130.146	13.44	11.946	25.386	192.824
SP kernel	4.964	12.078	17.042	129.334	14.144	12.386	26.53	208.096
RW kernel	9.162	20.006	29.168	217.684	17.814	22.36	40.174	385.726
NH kernel	5.348	11.264	16.612	141.18	12.568	11.714	24.282	190.376
GS kernel	6.444	16.748	23.192	178.434	17.216	15.344	32.56	272.744
Superv. GAT	5.278	10.892	16.17	108.636	12.81	11.978	24.788	159.324
Superv. GIN	5.106	10.766	15.872	116.174	12.792	11.394	24.186	173.72
Superv. GCN	4.942	10.312	15.254	105.194	12.392	11.84	24.232	159.356
GAE GAT	5.504	11.848	17.352	143.976	11.952	11.426	23.378	197.626
GAE GIN	5.4	12.002	17.402	143.182	12.554	11.738	24.292	201.638
GAE GCN	5.178	11.27	16.448	143.506	12.134	11.384	23.518	202.638
VGAE GAT	5.03	11.4	16.43	130.124	12.884	12.376	25.26	197.226
VGAE GIN	4.918	10.97	15.888	131.514	12.692	12.042	24.734	199.34
VGAE GCN	5.114	11.702	16.816	132.056	12.91	12.392	25.302	195.938
GFA GAT	5.07	11.564	16.634	131.582	12.988	12.412	25.4	198.78
GFA GIN	4.856	10.786	15.642	129.856	12.916	12.218	25.134	200.974
GFA GCN	5.03	11.432	16.462	132.046	12.696	12.338	25.034	201.038
ARVGA GAT	5.062	11.482	16.544	133.476	12.508	12.192	24.7	196.946
ARVGA GIN	4.894	10.912	15.806	128.944	12.234	11.794	24.028	198.654
ARVGA GCN	5.048	11.316	16.364	132.294	12.464	12.088	24.552	198.46

to predict the adjacency matrix A). All these models incorporate single-layer GCN, GAT, and GIN architectures in the encoder (and the decoder for GFA), employing AdamW optimizer with default parameters and a learning rate of 0.001, trained for 20 epochs with a batch size of 32.

GNNs and GAEs were implemented using PyTorch Geometric [9]. In all cases, cosine similarity was used as a measure for embedding similarity. For each scene graph in the dataset acting as the *query*, we retrieve the top k closest graphs with different PLACES-365 labels using a pretrained PLACES classifier with a ResNet50 backbone, resulting in slightly improved labels compared to [7]. We then evaluate whether the counterfactual graph, determined by the ground truth GED, is found within this ranked list of k items.

Evaluation Information retrieval metrics are used for evaluation, specifically Precision (P@k) and Normalized Discounted Cumulative Gain (NDCG@k). P@k returns the percentage of the relevant items, when considering the first k items in the rank. We also employ the “binary” variant from [7], where only the top-1 GED item is relevant, in line with the counterfactual logic. Binary NDCG@k compares the rank of the top-1 counterfactual returned by an algorithm to the ideal ground truth rank obtained by GED. While NDCG@k lacks direct interpretability, it’s widely used for comparing retrieval system performance. Our

evaluation focuses on $k=1, 2, 4$ ranks, once again emphasizing proximity to the top-1 result. Additional metrics assess the proposed edits' minimality by GNNs, including average node, edge, and overall edits, alongside average GED of counterfactuals. Lower values indicate better model performance, with these metrics considered relative to each other.

4.2 Quantitative Results

In Table 1, we present ranking results regarding counterfactual retrieval using all proposed graph models: graph kernels, supervised GNNs and unsupervised GAEs. For both dataset subsets, all supervised models were trained using 70K scene graph pairs extracted from $N=500$ graphs, while all unsupervised models were trained on the same 500 graphs (without pairing them).

Kernels reveal distinct performance patterns, with some closely rivaling unsupervised autoencoders. Notably, in VG-DENSE, SP and WL kernels excel, while in VG-RANDOM, WL and NH show superior performance. However, SP and NH metrics falter in VG-RANDOM and VG-DENSE, respectively, underscoring the significance of edge density. Conversely, kernels like RW consistently fail to retrieve counterfactual graphs, indicating their limitations in capturing graph structure. Supervised GNN models, particularly GCN, outperform kernels in ranking metrics, benefiting from optimized learning on ground truth GED. Unsupervised autoencoders exhibit more variability, with ARVGA GIN excelling in VG-DENSE and VG-RANDOM splits, underlining the importance of adversarial regularization for competitive performance.

In Table 2, we present results on the average number of edits, a common metric for evaluating counterfactual explanation systems, alongside the average top-1 counterfactual GED. In VG-DENSE experiments, the superior performance of supervised GCN is evident in edit numbers. While total edits appear similar across models, GFA GIN emerges as the second-best performer, indicating the limitations of relying solely on edit counts without considering their cost (GED). Comparing supervised GCN and GFA GIN, a significant gap in GED underscores their semantic divergence. Results for VG-RANDOM exhibit more variability, with GAE GAT leading in total edits. Considering both edit counts and GED provides insights into explanation minimality, highlighting the semantic relevance advantage of supervised models despite similar edit counts.

By comparing ranking metrics across the two dataset splits, we can easily observe that best results overall were achieved in the DENSE split. This is an expected behavior, since GNNs require interconnections for message passing procedures, i.e. to exchange and aggregate information from their neighbors.

Performance vs dataset size Although unsupervised GAEs lag behind supervised models, there is a notable discrepancy in the required ground truth data. Supervised GNNs necessitate training on $\sim N^2/2=70K$ pairs, maintaining a quadratic relationship with input data, entailing computationally expensive ground truth GED calculations. Conversely, unsupervised GAEs offer a more scalable solution, requiring N training samples without optimizing on ground

truth GED. This enables faster calculation of counterfactual explanations. While increasing training samples can enhance GAE performance, it may not be feasible in low-resource scenarios or where manual graph construction is required. Both approaches demonstrate computational efficiency, with GAE training taking less than 2 minutes for $N=500$ graphs, whereas supervised GNN training requires ~ 3 hours for $\sim N^2/2=70K$ graphs, with slight variations based on graph density. Despite differing training times, the retrieval, inference, and edit path computation times remain consistent between the two approaches. Training on a single GPU available in online platforms e.g. Kaggle or Google Colab is feasible for both supervised and unsupervised GNNs, while retrieval and inference operations are CPU-based, ensuring reproducibility of reported results.

4.3 Qualitative Results

Qualitative analysis is indispensable, particularly in the visual domain, where numerical metrics may not fully capture model performance. For graph retrieval, structural and semantic cues play vital roles. In Figure 3, we present results from top-performing models: supervised GCN, unsupervised ARVGA-GIN, and WL-kernel. Note that counterfactual classes do not need to align between models.

In the case of VG-DENSE, multiple instances exhibit concordance among models, owing to its dense interconnections and the inherent ability of all models to recognize matching structures. The 1st row demonstrates unanimous agreement, as the obtained scene graph essentially forms a subgraph of the query. A human could also agree on the semantic closeness between counterfactual instances: Semantics such as “table”, “cup”, “phone” are preserved, while the kitchen-related “cake” and “newspaper” should be edited to allow workstation-related semantics, such as “laptop”. Moving to the 2nd row, GNN methods align; successfully integrating structural and semantic information. Despite the kernel-retrieved result having a more similar structure, GNN methods successfully discern and retrieve an image featuring a cat on furniture, surpassing a mere depiction of a bed. In terms of human perception, counterfactuals depicting a “bedroom” (query) and a “living room” instance (GNN-based retrievals) respect the change of class label (“bedroom” \rightarrow “living room”) with minimally altering semantics (“pillow” and “cat” semantics are preserved), allowing effortless high-level interpretability. Conversely, in the 3rd row with a widespread disagreement, the merits of the supervised GNN network become evident. The unsupervised GAE captures an image resembling the query with a teddy bear wearing a bow but overlooks the presence of a dog. In contrast, the supervised GNN, having more accurately approximated GED, retrieves an image centered on a dog and a different type of toy. Interestingly, the kernel fails and retrieves an image of a train, emphasizing that a sole focus on structure (star subgraph) is insufficient.

Assessing retrieved VG-RANDOM results proves challenging due to the dissimilar nature of the sparser underlying graphs. In the 4th row, the supervised GCN retrieves a structurally closer scene graph, despite visual similarities in GNN-based counterfactuals. It becomes harder even for humans to evaluate their proximity, since all instances contain “chair” and “curtain” concepts, but no

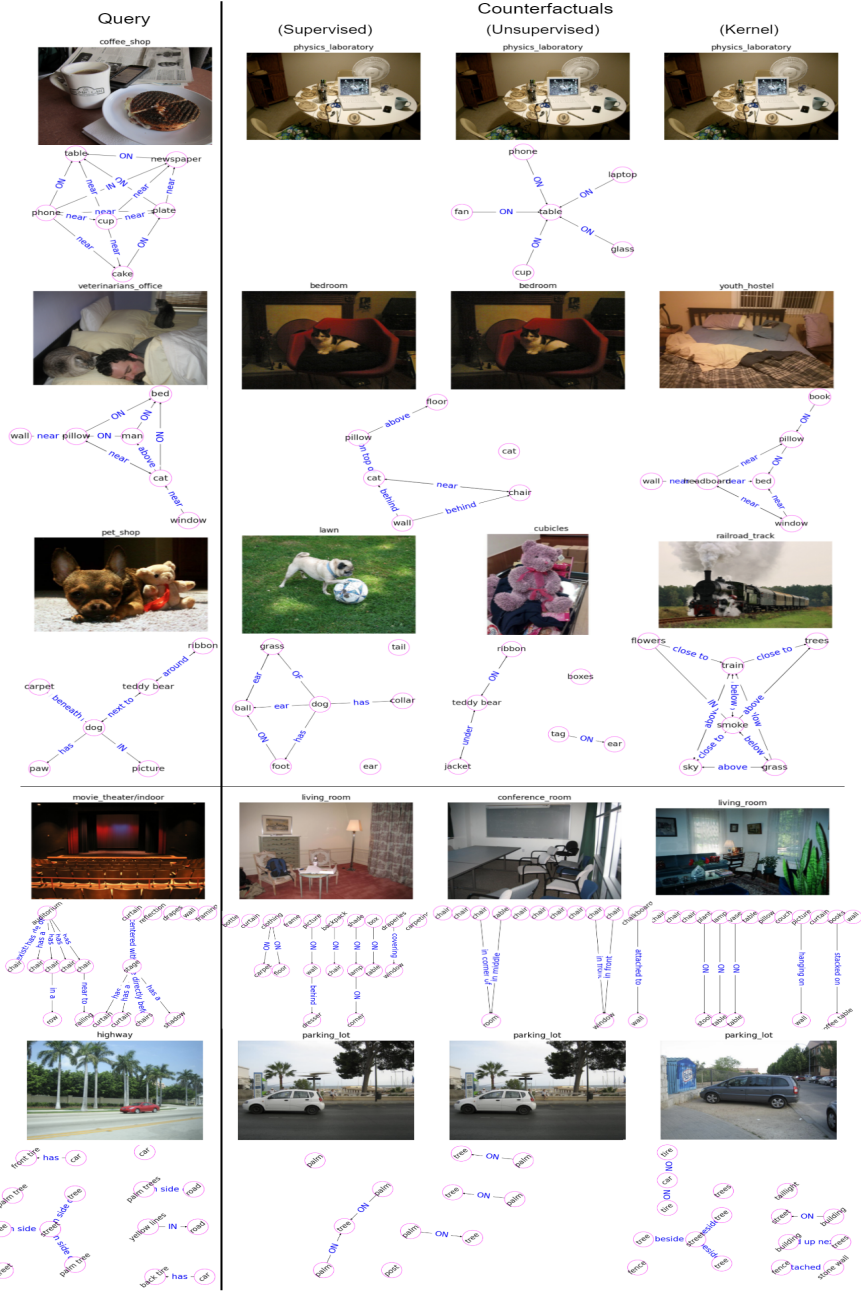


Fig. 3: Counterfactuals from the best supervised GNN, unsupervised GNN and kernel for VG-DENSE (top 3) and VG-RANDOM (bottom 2).

other discriminative structure or detail. In the final row the models reach consensus, successfully retrieving an image with palm trees, a characteristic the kernel fails to achieve despite the retrieval of very closely aligned graphs. The effectiveness of the framework relies on rich interconnections observed in VG-DENSE, underscoring the significance of expressive scene graphs, human intuition, and thoughtful data preprocessing for enhancing explanation informativeness.

Notably, none of the retrieved instances are misled by purely visual characteristics, such as color, contrast or brightness of images. This is because graph-based algorithms naturally disregard any such characteristics, as they are not integrated into scene graphs. Using the kitchen scenario as an example, the preservation of its identity through alterations like converting to grayscale or adjusting brightness suggests that graph machine learning models, particularly GNNs, can closely align with human perception.

5 Conclusion

In this work, we unify graph-based conceptual counterfactual explanation algorithms under a common framework, upon which we conduct a comparative study. Various graph-based algorithms, such as kernels, supervised and unsupervised GNNs, highlight the value of graph representations for counterfactuals, offering insights on what needs to be changed conceptually to transit to another class efficiently. Quantitative and qualitative analysis showcases the different criteria that influence the retrieval of counterfactual instances from varying graph algorithms, and the importance of well-defined and informative semantics towards human-interpretable explanations. There is ample room for further real-world applications of this framework within various domains where we have access to graph-structured data, such as recommendation systems, transportation networks, as well as agricultural and health inspection sectors.

Acknowledgments. This research work is Co-funded from the European Union’s Horizon Europe Research and Innovation programme under Grant Agreement No 101119714 — dAIry 4.0.

Disclosure of Interests. The authors have no competing interests to declare that are relevant to the content of this article.

References

1. Abid, A., Yuksekgonul, M., Zou, J.: Meaningfully debugging model mistakes using conceptual counterfactual explanations (2022)
2. Akula, A., Wang, S., Zhu, S.: Coccox: Generating conceptual and counterfactual explanations via fault-lines. Proceedings of the AAAI Conference on Artificial Intelligence **34**, 2594–2601 (04 2020). <https://doi.org/10.1609/aaai.v34i03.5643>
3. Augustin, M., Boreiko, V., Croce, F., Hein, M.: Diffusion visual counterfactual explanations (2022)

4. Browne, K., Swift, B.: Semantics and explanation: why counterfactual explanations produce adversarial examples in deep neural networks (2020)
5. Chang, C.H., Creager, E., Goldenberg, A., Duvenaud, D.: Explaining image classifiers by counterfactual generation (2019)
6. Dervakos, E., Thomas, K., Filandrianos, G., Stamou, G.: Choose your data wisely: A framework for semantic counterfactuals (2023)
7. Dimitriou, A., Lymperaiou, M., Filandrianos, G., Thomas, K., Stamou, G.: Structure your data: Towards semantic graph counterfactuals (2024)
8. Farid, K., Schrodi, S., Argus, M., Brox, T.: Latent diffusion counterfactual explanations. ArXiv **abs/2310.06668** (2023)
9. Fey, M., Lenssen, J.E.: Fast graph representation learning with PyTorch Geometric. In: ICLR Workshop on Representation Learning on Graphs and Manifolds (2019)
10. Filandrianos, G., Thomas, K., Dervakos, E., Stamou, G.: Conceptual edits as counterfactual explanations. In: Proceedings of the AAAI 2022 Spring Symposium on Machine Learning and Knowledge Engineering for Hybrid Intelligence (AAAI-MAKE 2022), Stanford University, Palo Alto, California, USA (21–23 March 2022)
11. Goyal, Y., Wu, Z., Ernst, J., Batra, D., Parikh, D., Lee, S.: Counterfactual visual explanations (2019)
12. Hasibi, R., Michoel, T.: A graph feature auto-encoder for the prediction of unobserved node features on biological networks (2020)
13. Hendricks, L.A., Hu, R., Darrell, T., Akata, Z.: Grounding visual explanations (2018)
14. Jonker, R., Volgenant, A.: A shortest augmenting path algorithm for dense and sparse linear assignment problems. Computing **38**(4), 325–340 (1987)
15. Kipf, T.N., Welling, M.: Semi-supervised classification with graph convolutional networks. arXiv preprint arXiv:1609.02907 (2016)
16. Kipf, T.N., Welling, M.: Variational graph auto-encoders (2016)
17. Kondor, R.: Diffusion kernels on graphs and other discrete structures. In: International Conference on Machine Learning (2002)
18. Krishna, R., Zhu, Y., Groth, O., Johnson, J., Hata, K., Kravitz, J., Chen, S., Kalantidis, Y., Li, L.J., Shamma, D.A., et al.: Visual genome: Connecting language and vision using crowdsourced dense image annotations. International journal of computer vision **123**(1), 32–73 (2017)
19. Li, Y., Gu, C., Dullien, T., Vinyals, O., Kohli, P.: Graph matching networks for learning the similarity of graph structured objects (2019)
20. Lymperaiou, M., Filandrianos, G., Thomas, K., Stamou, G.: Counterfactual edits for generative evaluation (2023)
21. Menis-Mastromichalakis, O., Liartis, J., Stamou, G.: Beyond one-size-fits-all: Adapting counterfactual explanations to user objectives. In: ACM CHI Workshop on Human-Centered Explainable AI (HCXAI) (2024)
22. Miller, G.A.: Wordnet: a lexical database for english. Communications of the ACM **38**(11), 39–41 (1995)
23. Miller, T.: Explanation in artificial intelligence: Insights from the social sciences. Artificial Intelligence **267**, 1–38 (2019). <https://doi.org/https://doi.org/10.1016/j.artint.2018.07.007>, <https://www.sciencedirect.com/science/article/pii/S0004370218305988>
24. Nikolentzos, G., Siglidis, G., Vazirgiannis, M.: Graph kernels: A survey. Journal of Artificial Intelligence Research **72**, 943–1027 (Nov 2021). <https://doi.org/10.1613/jair.1.13225>
25. OpenAI: Chatgpt: Conversational language model (2023)

26. OpenAI: Gpt-4 technical report. ArXiv **abs/2303.08774** (2023)
27. Pan, S., Hu, R., Long, G., Jiang, J., Yao, L., Zhang, C.: Adversarially regularized graph autoencoder for graph embedding (2019)
28. Poyiadzi, R., Sokol, K., Santos-Rodriguez, R., De Bie, T., Flach, P.: Face: Feasible and actionable counterfactual explanations. In: Proceedings of the AAAI/ACM Conference on AI, Ethics, and Society. AIES '20, ACM (Feb 2020). <https://doi.org/10.1145/3375627.3375850>
29. Rudin, C.: Stop explaining black box machine learning models for high stakes decisions and use interpretable models instead (2019)
30. Sanfeliu, A., Fu, K.S.: A distance measure between attributed relational graphs for pattern recognition. IEEE Transactions on Systems, Man, and Cybernetics **SMC-13**(3), 353–362 (1983). <https://doi.org/10.1109/TSMC.1983.6313167>
31. Vandenbende, S., Mahajan, D., Radenovic, F., Ghadiyaram, D.: Making heads or tails: Towards semantically consistent visual counterfactuals. arXiv preprint arXiv:2203.12892 (2022)
32. Veličković, P., Cucurull, G., Casanova, A., Romero, A., Lio, P., Bengio, Y.: Graph attention networks. arXiv preprint arXiv:1710.10903 (2017)
33. Wachter, S., Mittelstadt, B., Russell, C.: Counterfactual explanations without opening the black box: Automated decisions and the gdpr (2018)
34. Xu, K., Hu, W., Leskovec, J., Jegelka, S.: How powerful are graph neural networks? arXiv preprint arXiv:1810.00826 (2018)
35. Zeng, Z., Tung, A.K.H., Wang, J., Feng, J., Zhou, L.: Comparing stars: on approximating graph edit distance. Proc. VLDB Endow. **2**(1), 25–36 (aug 2009). <https://doi.org/10.14778/1687627.1687631>, <https://doi.org/10.14778/1687627.1687631>
36. Zhao, W., Oyama, S., Kurihara, M.: Generating natural counterfactual visual explanations. In: International Joint Conference on Artificial Intelligence (2020)
37. Zhou, B., Lapedriza, A., Khosla, A., Oliva, A., Torralba, A.: Places: A 10 million image database for scene recognition. IEEE Transactions on Pattern Analysis and Machine Intelligence (2017)